

circFOXMI1 contributes to sorafenib resistance of hepatocellular carcinoma cells by regulating MECP2 via miR-1324

Hanqin Weng,^{1,7} Lexiang Zeng,^{2,6,7} Linhui Cao,^{3,7} Tao Chen,¹ Yanshan Li,¹ Yunxiuxiu Xu,⁴ Yaorong Peng,^{5,6} and Yibiao Ye¹

¹Department of Hepato-Biliary Surgery, Dongguan People's Hospital, Southern Medical University, Dongguan 523000, China; ²Department of Traditional Chinese Medicine, Sun Yat-sen Memorial Hospital, Sun Yat-sen University, Guangzhou 510120, China; ³Department of Gastroenterology, Dongguan People's Hospital, Southern Medical University, Dongguan 523000, China; ⁴Department of Oncology, Dongguan People's Hospital, Southern Medical University, Dongguan 523000, China; ⁵Department of Hepato-Biliary Surgery, Sun Yat-sen Memorial Hospital, Sun Yat-sen University, Guangzhou 510120, China; ⁶Key Laboratory of Malignant Tumor Gene Regulation and Target Therapy of Guangdong Higher Education Institutes, Sun Yat-sen Memorial Hospital, Sun Yat-sen University, Guangzhou 510120, China

As one of the most common malignant tumors, hepatocellular carcinoma (HCC) is a leading cause of cancer-related deaths around the world. Emerging studies have indicated that circular RNAs (circRNAs), which play a crucial role in HCC pathogenesis and metastasis, are differentially expressed in HCC. However, the regulatory mechanisms of circRNA on sorafenib resistance of HCC are still unknown. In our study, we identified a novel circRNA, circFOXMI1, using RNA sequencing (RNA-seq) that was increased in sorafenib-resistant HCC tissues. Functionally, circFOXMI1 significantly inhibited HCC growth and enhanced sorafenib toxicity *in vitro*. Mechanistically, circFOXMI1 acted as a sponge of microRNA (miR)-1324, which is a negative regulator of MECP2, indicating that circFOXMI1 downregulation would regulate sorafenib resistance of HCC via releasing more free miR-1324 and suppressing MECP2 expression. Furthermore, miR-1324 overexpression was capable of reversing the circFOXMI1-induced malignant phenotypes and elevated expression of MECP2 in HCC cells. circFOXMI1 partially contributed to sorafenib resistance of HCC cells through upregulating MECP2 expression by sponging miR-1324.

INTRODUCTION

Hepatocellular carcinoma (HCC) is the most common pathological type (75%–85%) of primary liver cancer and is the 4th leading cause of cancer-related death worldwide.¹ However, the 5-year relative survival rate is approximately 18%, and the recurrence rate after surgery is as high as 65%–80%.² Although a multi-kinase inhibitor, sorafenib, has exhibited prominent clinical efficacy in HCC patients, poor prognosis of HCC is closely associated with the development of acquired resistance.^{3,4} Sorafenib resistance is one of the most important factors that restrict the long-term survival of HCC patients. Therefore, novel targets for reducing sorafenib resistance in HCC need to be developed.

Circular RNA (circRNA) is a novel non-coding RNA (ncRNA) with a highly conserved and stable covalently closed structure.⁵ circRNAs

are mostly derived from the gene's exon region, with a small portion formed by intron cleavage.⁶ circRNA functions in HCC were recently revealed⁷ and include competing endogenous RNAs (ceRNAs) or microRNA (miRNA) sponges and interactions with RNA-binding proteins and translating proteins.⁸ Because studies on the regulatory role of circRNAs in sorafenib resistance of HCC have not been reported, there are still great prospects to investigate the functions of circRNAs and the regulatory mechanism of sorafenib resistance in HCC.

Therefore, the principal purpose of our study was to reveal the significant role of circFOXMI1, which was markedly elevated in sorafenib-resistant HCC tissues and cell lines. circFOXMI1 is an important mediator of resistance to sorafenib in HCC. Furthermore, we illustrated that circFOXMI1 may act as a sponge of miR-1324 to upregulate the level of MECP2 and therefore promote drug resistance of HCC. Our study aimed to provide a potential prognostic biomarker for prognostic evaluation or a therapeutic target for the clinical treatment of HCC.

RESULTS

Profile of circRNAs in sorafenib-resistant HCC tissues

To investigate the expression profiles and regulatory effect of circRNAs, RNA-seq was performed in both sorafenib-resistant HCC cell lines (SR-HepG2 and SR-Huh7). By comparing the circRNA profiles between sorafenib-resistant and sorafenib-sensitive cells, a total of 269 most differentially expressing circRNAs (filtered by fold change

Received 4 September 2020; accepted 17 December 2020;
<https://doi.org/10.1016/j.omtn.2020.12.019>.

⁷Senior author

Correspondence: Yibiao Ye, Department of Hepato-Biliary Surgery, Sun Yat-sen Memorial Hospital, Sun Yat-sen University, Guangzhou 510120, China.
E-mail: drzhangtc66@163.com

Correspondence: Zaiguo Wang, Department of Hepato-Biliary Surgery, Dongguan People's Hospital, Southern Medical University, Dongguan 523000, China.
E-mail: YeYibiao@mail.sysu.edu.cn



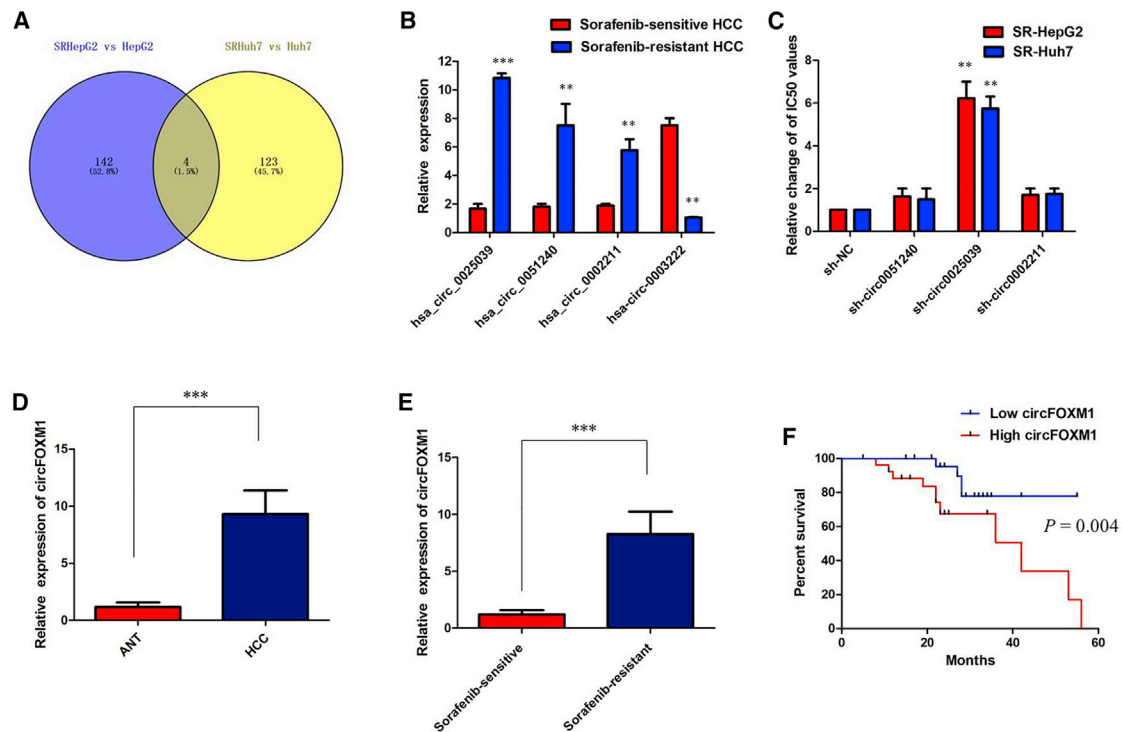


Figure 1. circRNA profiling in human sorafenib-resistant HCC cells and circFOXM1 characterization

(A) By comparing the circRNA profiles between sorafenib-resistant and sorafenib-sensitive cells, a total of 269 most differentially expressing circRNAs (filtered by $FC > 1.5$ and $FDR < 0.05$) were selected for overlap analysis. (B) The quantitative real-time PCR results indicated hsa-circ-0025039 (chr12:2975558-2977920) showed higher fold change in the sorafenib-resistant HCC tissues than in the sorafenib-sensitive tissues. (C) Knockdown of circFOXM1 reversed sorafenib resistance in both sorafenib-resistant HCC cell lines. (D) The qPCR results further confirmed that circFOXM1 was significantly increased in HCC tissues compared with ANT. (E) The qPCR results further confirmed that circFOXM1 was higher in sorafenib-resistant HCC tissues than in the sorafenib-sensitive tissues. (F) Patients with circFOXM1^{high} cell expression had a significantly worse prognosis than those with circFOXM1^{low}. All tests were performed at least three times. Data were expressed as mean \pm SD. *** $p < 0.001$; ** $p < 0.01$.

[$FC > 1.5$ and false discovery rate [$FDR < 0.05$] were selected for overlap analysis. As a result, four circRNAs (hsa-circ-0025039, hsa-circ-0051240, hsa-circ-0002211, and hsa-circ-0003222) were identified (Figure 1A). Among them, one circRNA was downregulated, while three circRNAs were upregulated. We then experimentally validated the three most upregulated circRNAs expression levels by quantitative real-time PCR using sorafenib-resistant and sorafenib-sensitive HCC tissue samples. The quantitative real-time PCR results indicated hsa-circ-0025039 (chr12:2975558-2977920) showed higher FC in the sorafenib-resistant HCC tissues than in the sorafenib-sensitive tissues (Figure 1B). By browsing the human reference genome (GRCh37/hg19), we knew that hsa_circ_0025039 was derived from the exon 4 and 5 of FOXM1 loci, and thus we named it circFOXM1 in this study. Furthermore, we found that knockdown of circFOXM1 reversed sorafenib resistance in SR-HepG2 and SR-Huh7 cells, while the other two circRNA showed little effect (Figure 1C).

To investigate the clinical significance of circFOXM1 expression in sorafenib sensitivity of HCC patients, the expression of circFOXM1 expression in 56 tumor tissues (31 sorafenib-sensitive HCC tissues and 25 sorafenib-resistant HCC tissues) and paired adjacent normal tissues (ANTs) were analyzed. The medians of circFOXM1 expres-

sion in tumor and adjacent tissues were calculated, respectively, which showed a higher expression level in tumorous tissues than in adjacent nontumorous tissues (Figure 1D), and its expression was higher in sorafenib-resistant HCC tissues than in the sorafenib-sensitive tissues (Figure 1E). Next, we explored the relationship between circFOXM1 expression and the clinicopathological characteristics of HCC patients, as listed in Table 1. The results showed that HCC patients with circFOXM1^{high} cells had larger tumors ($p = 0.031$), microvascular invasion ($p = 0.006$), and more advanced tumor stage ($p = 0.049$). Then, we explored the prognostic implications of circFOXM1 expression. Importantly, our results showed that patients with circFOXM1^{high} cell expression had a significantly worse prognosis than those with circFOXM1^{low}. These results indicate that circFOXM1 likely participates in the progression of HCC.

circFOXM1 silencing weakened sorafenib resistance in sorafenib-resistant HCC cells

To explore the biological functions of circFOXM1 in HCC, we measured circFOXM1 expression in HCC cell lines and normal liver cell line L02. circFOXM1 was markedly upregulated in sorafenib-resistant HCC cell lines compared with that in their parental HCC cell lines (Figure S1A). To confirm whether SR-HepG2 and SR-Huh7 cells were

Table 1. Correlation between circFOXM1 expression and clinicopathologic characteristics of HCC patients

Variable	circFOXM1		p value
	Low	High	
All cases	28	28	
Age, years, ≥ 50 : <50	16:12	14:14	0.789
Gender, male:female	10:18	16:12	0.179
HBsAg, positive:negative	19:9	14:14	0.277
Liver cirrhosis, with:without	16:12	10:18	0.179
AFP, $\mu\text{g/L}$, >20 : ≤ 20	14:14	16:12	0.789
Edmondson's grade, III + IV:I + II	9:19	18:10	0.014*
Tumor size, cm, >5 : ≤ 5	8:20	17:11	0.031*
Microvascular invasion, present:absent	10:18	21:7	0.006*
Encapsulation, incomplete:complete	14:14	16:12	0.789
TNM stage, II + III:I	14:14	22:6	0.049*
BCLC stage, B + C:A	10:18	21:7	0.006*

χ^2 test was used to test the association between two categorical variables. AFP, alpha-fetoprotein; BCLC, Barcelona Clinic Liver Cancer; HCC, hepatocellular carcinoma; HBsAg, hepatitis B surface antigen.
*Statistically significant.

resistant to sorafenib, Cell Counting Kit-8 (CCK-8) assay was performed to test IC_{50} of sorafenib. As shown in Figures 2A and 2B, IC_{50} values of sorafenib in SR-HepG2 and SR-Huh7 cells were significantly higher than those of their parental HepG2 and Huh7 cells ($p < 0.01$). Next, we designed two small hairpin RNA (shRNA) plasmids to target the unique back-splice junction. The back-splice junction-specific shRNAs (shcircFOXM1#1 and shcircFOXM1#2) had no effect on the level of FOXM1 mRNA in the SR-HepG2 and SR-Huh7 cells (Figure S1B). The quantitative real-time PCR analysis confirmed that circFOXM1 expression level was significantly downregulated in SR-HepG2 and SR-Huh7 cells by shcircFOXM1#1 instead of shcircFOXM1#2, so we chose shcircFOXM1#1 subsequently for the following experiments (Figure 2C; $p < 0.01$). Meanwhile, using the above-mentioned vector, we succeeded in overexpressing circFOXM1 in HepG2 and Huh7 cells. The quantitative real-time PCR assay indicated the relative abundance of circFOXM1 in HepG2 and Huh7 cells infected with circFOXM1 overexpression plasmid (Figure 2D; $p < 0.01$). Consistently, CCK-8 assay also implicated that knockdown of circFOXM1 rendered both SR-HepG2 and SR-Huh7 cells more sensitive to sorafenib-mediated cytotoxicity compared with the control group, as demonstrated by the decreased IC_{50} value of sorafenib following circFOXM1 downregulation (Figures 2E and 2F; $p < 0.01$). However, the opposite phenomenon was observed after overexpression of circFOXM1, and the IC_{50} values of sorafenib of HepG2 and Huh7 cells were significantly increased (Figures 2G and 2H; $p < 0.01$).

Additionally, we further evaluated whether the effect of circFOXM1 on sorafenib resistance of HCC cells was associated with cell apoptosis and cell cycle. SR-HepG2 and SR-Huh7 cells transfected with sh-circFOXM1#1 or sh-NC were treated with sorafenib ($3 \mu\text{M}$) for 24 h. Flow cytometry analysis results demonstrated that

circFOXM1 knockdown enhanced sorafenib-induced apoptosis in SR-HepG2 and SR-Huh7 cells with respect to the sh-NC group (Figure 3A; $p < 0.01$). However, cell apoptosis assays revealed that following overexpression of circFOXM1, the sorafenib-induced apoptosis of HepG2 and Huh7 cells was significantly decreased compared to the control group (Figure 3B; $p < 0.01$). The results of flow cytometry assays showed that circFOXM1 knockdown significantly increased the percent of cells in G0/G1 phase of SR-HepG2 and SR-Huh7 cells in the presence of sorafenib ($3 \mu\text{M}$) (Figures 3C and 3D; $p < 0.01$); however, overexpression of circFOXM1 significantly decreased the percent of cells in G0/G1 phase of HepG2 and Huh7 cells in the presence of sorafenib ($3 \mu\text{M}$) (Figures 3E and 3F; $p < 0.01$). Collectively, these results indicated that circFOXM1 silencing enhanced sorafenib-induced cytotoxicity in HCC cells.

Confirmation of subcellular localization of circFOXM1

We investigated the stability and localization of circFOXM1 in SR-HepG2 cells. Total RNAs from SR-HepG2 cells were isolated at the indicated time points after treatment with actinomycin D, an inhibitor of transcription. Analysis for stability of circFOXM1 and FOXM1 in SR-HepG2 cells treated with actinomycin D, an inhibitor of transcription, revealed that the half-life of the circFOXM1 transcript exceeded 24 h, which was more stable than FOXM1 (Figure 4A). According to the degradation effect of RNase R on linear RNA and the inhibitory effect of actinomycin D on RNA transcription, the degradation of linear FOXM1 was significantly faster than that of circFOXM1 in SR-HepG2 cells, indicating that the stability of circFOXM1 was increased because of its circular structure (Figure 4B). We then investigated the localization of circFOXM1. The quantitative real-time PCR of RNAs from nuclear and cytoplasmic fractions indicated that circFOXM1 was predominantly localized in the cytoplasm of SR-HepG2 cells (Figure 4C). Our results implied that circFOXM1 harbored a loop structure and was predominantly localized in the cytoplasm.

circFOXM1 serves as a sponge for multiple miRNAs

An increasing number of studies have reported that circRNAs act as miRNA sponges; therefore, we investigated whether circFOXM1 has the ability to bind to miRNAs. Through StarBase v3.0, we found that 12 miRNAs were predicted to be possible targets of circFOXM1. To verify the critical functional miRNAs that may interact with circFOXM1 in HCC cells, a circFOXM1-specific probe was used to perform RNA *in vivo* precipitation (RIP) in SR-HepG2 cells, which were then screened by the qRT-PCR for the potential miRNAs that had been predicted. Using RIP circFOXM1 pull-down experiments, we purified circFOXM1-associated RNAs and analyzed 12 candidate miRNAs in the complex. The results showed a specific enrichment of circFOXM1 and miR-1324 compared to the negative control (NC) probe, whereas the other miRNAs were slightly enriched or not enriched, indicating that miR-1324 is one of the critical circFOXM1-associated miRNAs in HCC cells (Figure 5A). Next, we performed RNA immunoprecipitation (RIP) with argonaute 2 (AGO2) antibody in SR-HepG2 cells. Our results showed that circFOXM1 and miR-1324, but not circANRIL (a circular RNA that reportedly does not bind to AGO2), were significantly enriched, as they were precipitated

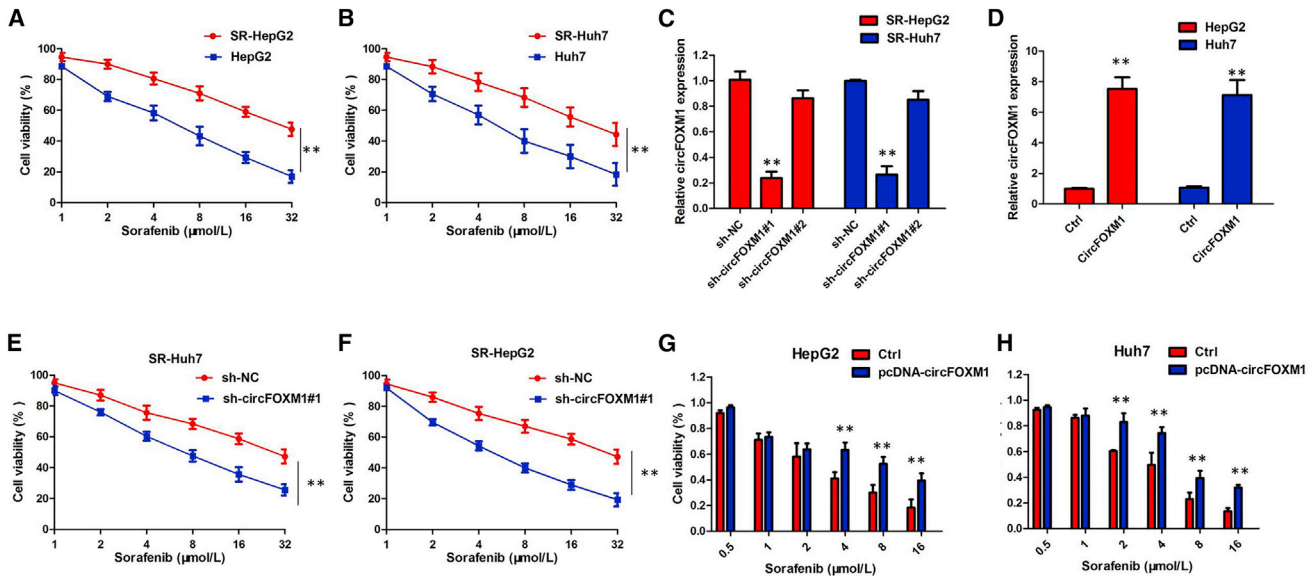


Figure 2. circFOXM1 silencing weakened sorafenib resistance in sorafenib-resistant HCC cells

(A) IC₅₀ values of sorafenib in SR-HepG2 cells were significantly higher than those of their parental HepG2 cells. (B) IC₅₀ values of sorafenib in SR-Huh7 cells were significantly higher than those of their parental Huh7 cells. (C) The expression of circFOXM1 was downregulated by si-circFOXM1 in SR-HepG2 and SR-Huh7 cells. (D) circFOXM1 was significantly upregulated after transfecting the circFOXM1 expression vector in HepG2 and Huh7 cells. (E) CCK-8 assay also implicated that knockdown of circFOXM1 rendered SR-HepG2 cells more sensitive to sorafenib-mediated cytotoxicity compared with the control group. (F) CCK-8 assay also implicated that knockdown of circFOXM1 rendered SR-Huh7 cells more sensitive to sorafenib-mediated cytotoxicity compared with the control group. (G) The IC₅₀ value of sorafenib in HepG2 cells was significantly increased after overexpression of circFOXM1. (H) The IC₅₀ value of sorafenib in Huh7 cells was significantly increased after overexpression of circFOXM1. All tests were performed at least three times. Data were expressed as mean \pm SD. * p < 0.05, ** p < 0.01.

by the AGO2 antibody (Figure 5B). These results indicated that circFOXM1 may act as a binding platform for AGO2 and miR-1324. To verify these results, we performed a luciferase assay using miR-1324 mimics co-transfected with luciferase reporters (which contained a wild-type [WT] or miR-1324-target mutant circFOXM1 sequence) into HEK293 T cells. Compared with the NC RNA, miR-1324 decreased the luciferase reporter activity significantly in the cells with the wild-type circFOXM1 sequence but not the cells with either the WT- or the miR-1324-target mutant circFOXM1 sequence (Figures 5C and 5D). Furthermore, using a pull-down assay with biotinylated miR-1324 mimics, we observed significant enrichment of circFOXM1 compared with the level in the NCs, while circANRIL was not enriched in the SR-HepG2 cells (Figure 5E). In addition, miR-1324 did not show significant changes after circFOXM1 was silenced, and circFOXM1 did not show significant changes after miR-1324 expression was upregulated (Figures 5F and 5G). These findings indicate that circFOXM1 and miR-1324 are likely not degraded by each other. All of the above experiments confirmed that circFOXM1 may function as a sponge for miR-1324 in HCC cells.

circFOXM1 positively regulated MECP2 expression by interacting with miR-1324 in HCC cells

Through overlapping the results of miRNA target prediction by miR-Walk, TargetScan, mirDIP, and miRDB, the 3' UTRs of 4 candidates (MECP2, ZNRF1, ETF1, and CPLX4) were considered as putative tar-

gets of miR-1324 (Figure 6A). However, we did not detect significant changes in the expression levels of these mRNAs in SR-HepG2 cells transfected with a miR-1324 mimic or in HepG2 cells transfected with a miR-1324 inhibitor, except for the expression of the MECP2 (Figures 6B and 6C; p < 0.01). To verify whether the 3' UTR of MECP2 mRNAs were targets of miR-1324 in the HCC cells, a pLG3 luciferase reporter gene assay was used. The WT 3' UTR sequence and the mutant (mu) 3' UTR sequence of MECP2 were cloned and placed into a pLG3 luciferase reporter vectors. The luciferase activity was significantly inhibited by the miR-1324 mimics in the HEK293 T cells transfected with the WT 3' UTR sequence. The luciferase activity was not changed by the miR-1324 mimics in the HEK293 T cells transfected with the mu 3' UTR sequence (Figure 6D; p < 0.01). Furthermore, we found that circFOXM1 knockdown triggered a substantial decline of MECP2 mRNA and protein level in SR-HepG2 cells. Moreover, circFOXM1 knockdown-mediated decrease of MECP2 expression was significantly recuperated following miR-1324 inhibitor (Figures 6E and 6F). All of these data led to the conclusion that circFOXM1 positively regulated MECP2 expression by interacting with miR-1324 in sorafenib-resistant HCC cells.

DISCUSSION

In the current study, we investigated the role of circFOXM1 on sorafenib resistance of HCC and demonstrated the regulatory mechanism of miR-1324/MECP2 signaling pathway. Our data suggested

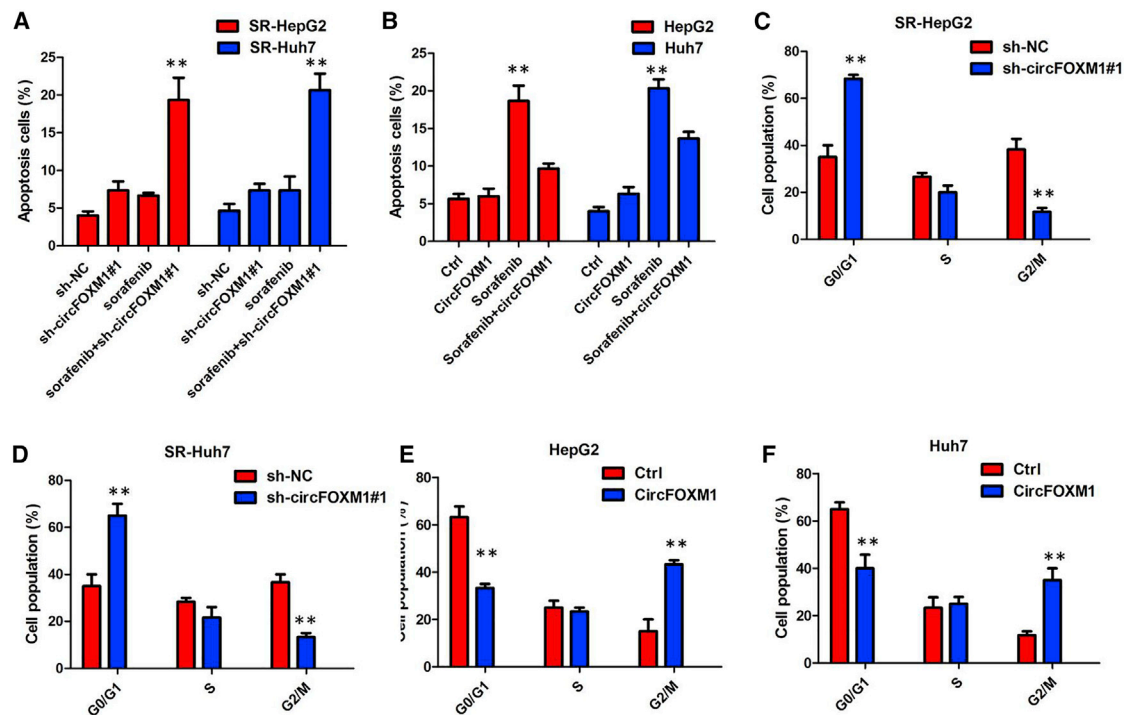


Figure 3. The effect of circFOXM1 on sorafenib resistance of HCC cells was associated with cell apoptosis and cell cycle

(A) circFOXM1 knockdown enhanced sorafenib-induced apoptosis in SR-HepG2 and SR-Huh7 cells with respect to the sh-NC group. (B) The sorafenib-induced apoptosis of HepG2 and Huh7 cells was significantly decreased compared to the control group after overexpression of circFOXM1. (C) circFOXM1 knockdown significantly increased the percent of cells in G0/G1 phase of SR-HepG2 cells in the presence of sorafenib. (D) circFOXM1 knockdown significantly increased the percent of cells in G0/G1 phase of SR-Huh7 cells in the presence of sorafenib. (E) Overexpression of circFOXM1 significantly decreased the percent of cells in G0/G1 phase of HepG2 cells in the presence of sorafenib. (F) Overexpression of circFOXM1 significantly decreased the percent of cells in G0/G1 phase of Huh7 cells in the presence of sorafenib. All tests were performed at least three times. Data were expressed as mean \pm SD. ** $p < 0.01$.

that circFOXM1 knockdown could increase the sorafenib sensitivity of HCC cells. circFOXM1 could serve as a molecular sponge of miR-1324, which weakens the inhibitory effect of miRNA on the downstream target gene MECP2. Furthermore, dual-luciferase reporter system and RIP assay verified the direct interaction of circFOXM1, miR-1324, and MECP2. These results indicated that silencing circFOXM1 could increase the sensitivity of HCC cells to sorafenib, thus suppressing tumor development.

For patients with advanced liver cancer, the emergence of sorafenib has brought new hope to their treatment. Acquired resistance, however, often happens within 6 months, and only 30% of HCC patients could benefit from sorafenib. Such high incidence of resistance has greatly limited its clinical application, while the underlying mechanisms of sorafenib resistance in HCC have not been well characterized. circRNAs are a large class of ncRNAs that are composed of special exonic sequences in the absence of a free 3' or 5' end.⁹ circRNAs act as tumor suppressors or oncogenes to participate in the development of a variety of tumors and are becoming novel diagnostic and prognostic biomarkers.¹⁰ They can also serve as ceRNAs through the combination of their complementary miRNA response elements (MREs) and the primary miRNAs, exerting positive or negative

effects on the processing and expression of mature mRNAs, thus indirectly involved in various progress of physiological processes.¹¹ circRNAs have been identified as diagnostic or predictive biomarkers of various diseases, especially cancers, in recent years by an increasing number of studies.¹² However, the roles of circRNAs in drug resistance of HCC are still unclear.

To address this question, we initially detected the profile of circRNAs in both sorafenib-resistant HCC cell lines (SR-HepG2 and SR-Huh7) using RNA-seq and found that circFOXM1 expression was aberrantly upregulated in sorafenib-resistant HCC cells. Then, we found that circFOXM1 was upregulated in HCC tissues, and patients with high circFOXM1 expression were prone to have a higher incidence of tumor metastasis and poorer prognosis. In line with HCC tissues, circFOXM1 was prominently upregulated in two sorafenib-resistant HCC cell lines in comparison to their parental counterparts. In addition, *in vitro* loss/gain-of-function assays illustrated that circFOXM1 inhibited sorafenib sensitivity in HCC cells and facilitated HCC cell proliferation. These results demonstrated that circFOXM1 functions as an oncogene that plays an important role in the development of sorafenib resistance in HCC cells through promoting multiple malignant phenotypes.

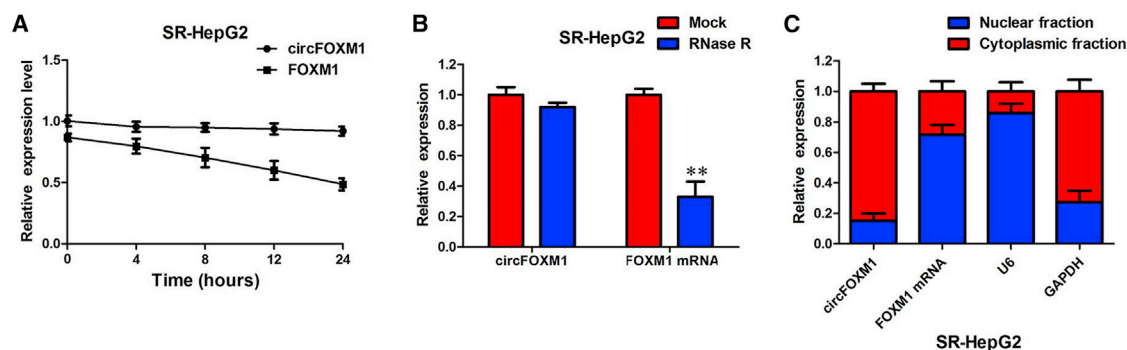


Figure 4. Confirmation of subcellular localization of circFOXM1

(A) Quantitative real-time PCR for the abundance of circFOXM1 and FOXM1 in SR-HepG2 cells treated with actinomycin D at the indicated time point. (B) Quantitative real-time PCR for the expression of circFOXM1 and FOXM1 mRNA in SR-HepG2 cells treated with or without RNase R. (C) Levels of circFOXM1 in the nuclear and cytoplasmic fractions of SR-HepG2 cells. Data were expressed as mean \pm SD. ** $p < 0.01$.

It has been reported that circRNAs can absorb miRNA and overcome the original repression on the miRNA-targeted gene by functioning as a post-transcriptional regulator (miRNA sponge), which is deemed as ceRNA in the cytoplasm.¹³ Herein, we predicted and subsequently confirmed that miR-1324 could interact directly with circFOXM1 using luciferase reporter assay, RIP, and RNA pull-down assays. Some reports revealed that miR-1324 could inhibit cell proliferation, induce cell apoptosis, and reduce cell migration and invasion by targeting multiple oncogenes in laryngeal squamous cell carcinoma, papillary thyroid cancer, glioma, and non-small cell lung cancer.^{14–17} Our results showed that miR-1324 acts as a tumor suppressor in HCC, consistent with those of previous reports. The reciprocal regulation between circFOXM1 and miR-1324 was validated in our current study. Knockdown of circFOXM1 significantly affected miR-1324 expression. Moreover, our data demonstrate that the knockdown of circFOXM1 promoted sensitivity of HCC cells to sorafenib by upregulating miR-1324.

Next, we explored targets of miR-1324 and confirmed MECP2 as a functional target of miR-1324 in HCC. MECP2 is known to prompt oncogenic and metastatic programs in addition to its proliferative and apoptotic functions.¹⁸ Li et al.¹⁹ found that MeCP2 was expressed significantly higher in HCC tissues compared with cirrhosis and non-cirrhosis tissues. MeCP2 could be a novel risk marker to predict HCC development in CHB patients with profound viral suppression under NA therapy. MeCP2 measurement may serve as a useful strategy for risk stratification in terms of follow-up interval and HCC surveillance.^{19–22} We found that circFOXM1 could promote MECP2 expression by competitively sponging miR-1324, uncovering the ceRNA network of circFOXM1/miR-1324/MECP2 in HCC.

In conclusion, our study on the oncogenic role of circFOXM1 in sorafenib resistance of HCC showed that circFOXM1 knockdown in sorafenib-resistant HCC cells could increase their sensitivity to sorafenib treatment both *in vitro* and *in vivo*, possibly by regulating the miR-1324/MECP2 axis as a ceRNA. This study elucidated a new

mechanism for development of HCC and indicated a novel target for treatment of HCC.

MATERIALS AND METHODS

Patients and tissues

Pairs of fresh HCC tissues and ANTs were collected from 56 HCC patients at the Department of Hepato-Biliary Surgery, Dongguan People's Hospital, Southern Medical University between 2014 and 2019. Tumor specimens and corresponding ANTs were collected and stored in liquid nitrogen until use. After completion of 2 cycles of sorafenib-based adjuvant target therapy, patients were divided into sorafenib-sensitive ($n = 31$) and sorafenib-resistant groups ($n = 25$). All tumor specimens were obtained by surgical resection prior to undergoing target therapy. The study was approved by the Ethics Committee of Southern Medical University, and written informed consent was obtained from each patient prior to surgery.

Cell culture and reagents

HCC cell lines HepG2, Huh-7, and the normal human liver cell line LO2 were purchased from the Chinese Academy of Sciences Cell Bank Type Culture Collection. The cells were cultured with DMEM and RPMI-1640 (Gibco, Carlsbad, CA, USA) together with 10% fetal bovine serum (Gibco) at 37°C in an atmosphere containing 5% CO₂. Sorafenib (BAY 43-9006) was contributed by MedChem Express. Sorafenib was dissolved in DMSO with a final concentration of DMSO <0.1%. To generate sorafenib-resistant hepatoma cells, HepG2 and Huh-7 cells were cultured with 1 mmol/L sorafenib. The concentration was slowly increased by 0.5 mmol/L per month (up to 5 mmol/L). After more than 10 months, two sorafenib-resistant cell lines were obtained and named sorafenib-resistant HepG2 (SR-HepG2) and sorafenib-resistant Huh7 (SR-Huh7).

Analyzing the circRNA expression profile

Total RNA from parental sorafenib-resistant and sorafenib-sensitive HCC cells was extracted with TRIzol reagents (Invitrogen, Carlsbad, CA, USA), as per the manufacturer's protocol. The rRNA was

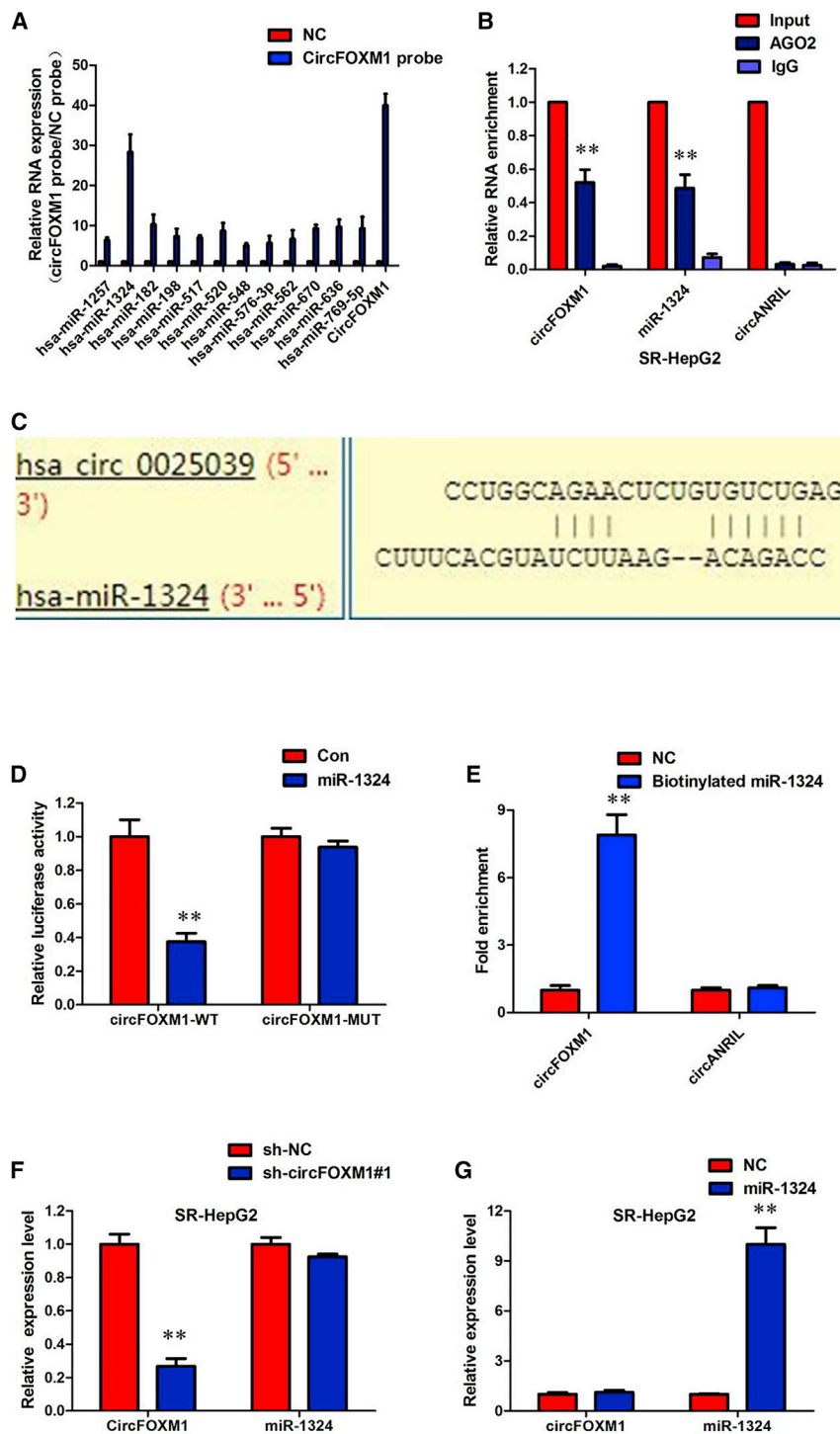


Figure 5. circFOXM1 functioned as a molecular sponge of miR-1324 in HCC cells

(A) RIP was performed for circRNA in SR-HepG2 cells using a circFOXM1 probe and a negative control (NC) probe. (B) RIP experiments were carried out using an AGO2 antibody with HCC cell extracts. (C) The binding sequence between miR-1324 and circFOXM1. (D) The luciferase reporter systems showed that miR-1324 mimic considerably reduced the luciferase activity of the WT-circFOXM1 luciferase reporter vector compared with NC, while miR-1324 mimic did not pose any impact on the luciferase activity of MUT-circFOXM1-transfected cells. (E) The level of circFOXM1 in the streptavidin-captured fractions of the HCC cell lysates after transfection with biotinylated miR-1324 or the NC. circANRIL was used as a NC. (F) miR-1324 did not show significant changes after circFOXM1 was silenced. (G) circFOXM1 did not show significant changes after miR-1324 expression was up-regulated. All tests were performed at least three times. Data were expressed as mean ± SD. **p < 0.01.

using the NEBNext Ultra RNA Library Prep Kit from Illumina (New England Biolabs, Beverly, MA, USA), and they were subjected to deep sequencing with an Illumina HiSeq 3000 at Ri-boBio (Guangzhou, China).

Identification and quantification of circRNAs

The RNA-seq FASTQ reads were first mapped to a human reference genome (GRCh37/hg19) using TopHat2.50. The unmapped reads were then used to identify circRNAs as previously described. Differential expression analysis of circRNAs was executed using R software package DEGseq. Only the circRNAs that were differently expressed with a q value < 0.05 were chosen for further analysis. The FC was log₂ transformed, and we used a log₂ (FC) >1.5 (or < -1.5) and a q value <0.05 to sort the differently expressed circRNAs. Subsequently, to generate an overview of circRNA expression profiles between the two groups, hierarchical clustering analysis was performed.

RNA preparation and quantitative real-time PCR

Total RNA extraction and quantification, RNA purification, and cDNA synthesis were performed. 2 μg total RNA was incubated for

removed from approximately 2 μg total RNA from each sample by using the Epicenter Ribo-Zero rRNA Removal Kit (Illumina, USA), followed by RNase R treatment (Epicenter Technologies, Madison, WI, USA). Subsequently, strand-specific RNA-seq libraries were prepared

15 min at 37°C with or without 3 U/μg RNase R (Epicenter Technologies, WI, USA) for RNase R treatment. Quantitative real-time PCR was performed with PowerUp SYBR Green Master Mix (Thermo Fisher, MA, USA) and the Applied Biosystems StepOnePlus Real-

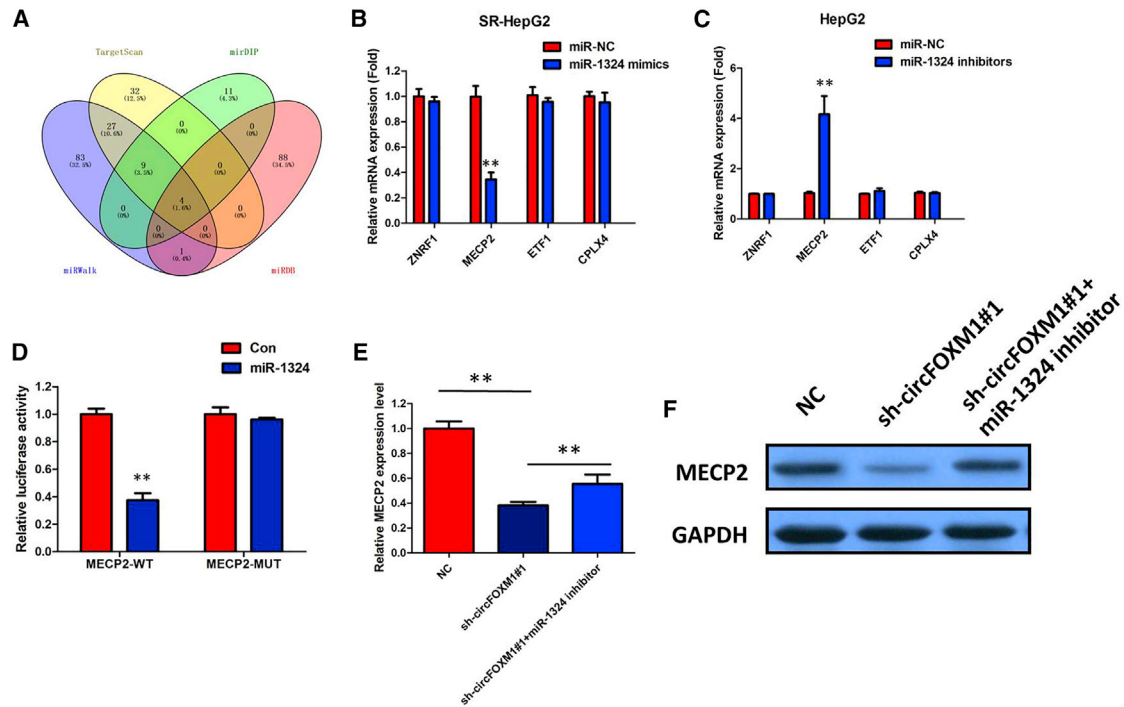


Figure 6. circFOXM1 positively regulated MECP2 expression by interacting with miR-1324 in HCC cells

(A) Venn diagram showing 4 genes that are putative miR-1324 targets computationally predicted by four algorithms (miRWalk, TargetScan, mirDIP, and miRDB). (B) mRNA levels of 4 candidate target genes were detected in SR-HepG2 cells transfected with a miR-1324 mimic. (C) mRNA levels of 4 candidate target genes were detected HepG2 cells transfected with a miR-1324 inhibitor. (D) miR-1324 mimics led to decreased fluorescence of the wild-type MECP2 3' UTR but had no effect on the mutant vectors. (E) Inhibition of circFOXM1-mediated decrease of MECP2 mRNA expression was significantly recuperated following miR-1324 inhibitors. (F) Inhibition of circFOXM1-mediated decrease of MECP2 protein expression was significantly recuperated following miR-1324 inhibitors. All tests were performed at least three times. Data were expressed as mean \pm SD. ** $p < 0.01$.

Time PCR Detection System (Life Technologies, CA, USA) to detect RNA expression. To calculate the relative gene expression, the $2^{-\Delta\Delta CT}$ method normalized to GAPDH was used, and the FC of gene expression was calculated by the $2^{-\Delta\Delta CT}$ method. Bulge-loop miRNA quantitative real-time PCR Primer Sets (one RT primer and a pair of qPCR primers for each set) specific for miR-1324 were designed by RiboBio (Guangzhou, China). The relative expression of miR-1324 was normalized to human U6 snRNA.

Cell transfection

Knocked down or overexpressed circFOXM1 transfection experiment shRNAs targeting the junction region of the circFOXM1 sequence and circFOXM1-overexpressing lentivirus were synthesized by Hanbio Company (Shanghai, China). HCC cell lines were transfected with circFOXM1 shRNA or the circFOXM1-overexpressing lentivirus according to the manufacturer's instructions. The miRNA mimics, inhibitor, and small interfering RNAs (siRNAs) were obtained from GenePharma (Shanghai, China). For transient transfection, cells were transfected with Lipofectamine 2000 reagent (Invitrogen, Carlsbad, CA, USA), according to the manufacturer's instructions. For stable cell line establishment, the lentiviral vector was introduced into HEK293T cells by transient transfection. After 6 h, the cell culture

medium was replaced, and viral supernatants were collected 48 h later. The supernatant was then collected and filtered through a 0.22- μ m filter. Cells were infected at approximately 70% confluence in complete medium supplemented with 8 μ g/mL polybrene (Sigma), followed by selection with puromycin at 0.5 μ g/mL (Sigma). The overexpression efficiency was determined by quantitative real-time PCR.

Cell proliferation assay

CCK-8 assay (Dojindo, Japan) was used as previously described. Briefly, transfected cells were seeded into 96-well plates (3,000 cells/well) and incubated overnight. Cells were then treated with sorafenib at various concentrations for 24 h. To test the cell proliferation, 10 μ L of CCK-8 reagent was added to each well and incubated for 2 h at 37°C. Then, the absorption was evaluated by a microplate reader at 450 nm (Tecan, Switzerland).

Cell cycle and apoptosis assay

Cells were seeded into 6-well plates and treated with sorafenib for 24 h. 3×10^5 treated cells were seeded into 6-well plates and cultured for 48 h at 37°C to assess the cell cycle and apoptosis. The cells for cell cycle analysis were digested using trypsin (Hyclone), washed twice

with phosphate-buffered saline (PBS), and fixed in 70% ethanol overnight at 4°C. Then the cells were centrifuged at $500 \times g$ for 5 min, washed twice with cold PBS, and centrifuged. Cell cycle analysis was performed through fluorescence-activated cell sorting flow cytometry (Beckman Coulter, Palo Alto, CA, USA) after treating the cells with RNase A (0.1 mg/mL) and propidium iodide (PI, 0.05 mg/mL) purchased from 4A Biotech (Beijing, China) for 30 min at 37°C. Following the instructions of the manufacturer, cells were harvested and were stained with Annexin V-FITC/PI (KeyGEN Biotech, Nanjing, China) for the analysis of apoptosis. Then the cells were acquired by flow cytometry (FACScan, BD Biosciences, USA) and analyzed by FlowJo 7.6.1.

Actinomycin D and RNase R treatment

Transcription was inhibited by adding actinomycin D (2 mg/mL) or DMSO (Sigma-Aldrich, St. Louis, MO, USA) as a control to the culture medium. Total RNA (5 µg) was incubated with or without 3 U/µg RNase R (Epicenter Technologies) at 37°C for 30 min, and the resulting RNA was purified using an RNeasy MinElute Cleaning Kit (QIAGEN, Germany). After the treatment above, RNA was transcribed into cDNA, and the expression levels of GAPDH and circFOXM1 were determined by quantitative real-time PCR.

Cell fractionation assay

Cytoplasmic and nuclear RNA were acquired using a Cytoplasmic and Nuclear RNA Purification Kit (Invitrogen, CA, USA). Briefly, the cells were harvested and incubated for 10 min with lysis solution on ice, then centrifuged for 3 min at $12,000 \times g$. The supernatant was collected for cytoplasmic RNA, and the nuclear pellet was used for nuclear RNA extraction. GAPDH was used as the cytoplasmic endogenous control and U6 small nuclear RNA as the nuclear endogenous control.

In vivo circRNA precipitation, RIP, and luciferase reporter assays

Biotin-labeled circFOXM1 and NC probes were synthesized by the GeneChem Company. In brief, cells were washed with cold PBS, fixed with 1% formaldehyde, lysed in co-immunoprecipitation (coIP) buffer, sonicated, and centrifuged. Then, the supernatant was cultured with M280 streptavidin Dynabeads (Invitrogen) mixture and incubated at 30 °C for 12 h. Subsequently, the mixture was washed and incubated with lysis buffer and proteinase K. RNA was extracted from the mixture using TRIzol Reagent (Invitrogen). The RIP assay was carried out using a Magna RIP RNA-binding protein immunoprecipitation kit (Millipore). In brief, cell lysates were cultured with Dynabeads coated with AGO2 antibody or IgG antibody at 4 °C for 12 h, and total RNA was extracted for the detection of enriched circFOXM1 and miRNA by qRT-PCR.

For the luciferase reporter assay, cells (5×10^3) were seeded into 96-well plates and co-transfected with corresponding plasmids and microRNA mimics or inhibitors using the Lipofectamine 2000 transfection reagent. Luciferase activity was measured using the dual-luciferase reporter assay system (Promega, Madison, WI, USA) after 48 h of incubation following the manufacturer's instructions. Independent experiments were per-

formed in triplicate. Relative luciferase activity was normalized to the Renilla luciferase internal control.

Western blot assay

The lysates from cells were collected by RIPA buffers (Beyotime Biotechnology, Shanghai, China) and boiled for 5 min at 100°C. Then, the proteins were transferred to polyvinylidene fluoride (PVDF) membrane and blocked by non-fat dried milk. The membrane was incubated with primary antibodies at 4°C overnight. On the following day, the membrane was washed strictly and probed with horseradish peroxidase (HRP)-conjugated secondary antibody, followed by visualization with ECL Plus chemiluminescence reagent (Beyotime Biotechnology).

Statistical analysis

Variables were expressed in mean \pm standard deviation. To measure the difference between two groups, Student's t test was performed. One-way ANOVA was employed to measure differences between more than two groups. p values <0.05 were considered statistically significant.

Availability of data and materials

The datasets supporting the conclusions of this article are included within the article and [Supplemental information](#).

Consent for publication

We have received consent from individual patients who have participated in this study. The consent forms will be provided upon request.

SUPPLEMENTAL INFORMATION

Supplemental Information can be found online at <https://doi.org/10.1016/j.omtn.2020.12.019>.

ACKNOWLEDGMENTS

The authors received funding from Provincial Basic and Applied Basic Research Project (Provincial Natural Fund) Doctor startup project (2016A030310089).

AUTHOR CONTRIBUTIONS

H.W. and Z.W. performed primer design and experiments. L.C. and Y.Y. contributed flow cytometry assay and animal experiments. X.C. and L.Y. collected and classified the human tissue samples. W.F. and L.L. contributed to quantitative real-time PCR. Y.Y. analyzed the data. H.W. wrote the paper. All authors read and approved the final manuscript.

DECLARATION OF INTERESTS

The authors declare no competing interests.

REFERENCES

1. Siegel, R., Desantis, C., and Jemal, A. (2014). Colorectal cancer statistics, 2014. *CA Cancer J. Clin.* 64, 104–117.
2. Hernandez-Gea, V., Toffanin, S., Friedman, S.L., and Llovet, J.M. (2013). Role of the microenvironment in the pathogenesis and treatment of hepatocellular carcinoma. *Gastroenterology* 144, 512–527.

3. Bruix, J., Reig, M., and Sherman, M. (2016). Evidence-based diagnosis, staging, and treatment of patients with hepatocellular carcinoma. *Gastroenterology* 150, 835–853.
4. Llovet, J.M., Montal, R., Sia, D., and Finn, R.S. (2018). Molecular therapies and precision medicine for hepatocellular carcinoma. *Nat. Rev. Clin. Oncol.* 15, 599–616.
5. Qu, S., Yang, X., Li, X., Wang, J., Gao, Y., Shang, R., Sun, W., Dou, K., and Li, H. (2015). Circular RNA: A new star of noncoding RNAs. *Cancer Lett.* 365, 141–148.
6. Salmena, L., Poliseno, L., Tay, Y., Kats, L., and Pandolfi, P.P. (2011). A ceRNA hypothesis: the Rosetta Stone of a hidden RNA language? *Cell* 146, 353–358.
7. Memczak, S., Jens, M., Elefsinioti, A., Torti, F., Krueger, J., Rybak, A., Maier, L., Mackowiak, S.D., Gregersen, L.H., Munschauer, M., et al. (2013). Circular RNAs are a large class of animal RNAs with regulatory potency. *Nature* 495, 333–338.
8. Patop, I.L., and Kadener, S. (2018). circRNAs in Cancer. *Curr. Opin. Genet. Dev.* 48, 121–127.
9. Yin, Y., Long, J., He, Q., Li, Y., Liao, Y., He, P., and Zhu, W. (2019). Emerging roles of circRNA in formation and progression of cancer. *J. Cancer* 10, 5015–5021.
10. Zhang, Y., Liang, W., Zhang, P., Chen, J., Qian, H., Zhang, X., and Xu, W. (2017). Circular RNAs: emerging cancer biomarkers and targets. *J. Exp. Clin. Cancer Res.* 36, 152.
11. Zhang, Z., Xie, Q., He, D., Ling, Y., Li, Y., Li, J., and Zhang, H. (2018). Circular RNA: new star, new hope in cancer. *BMC Cancer* 18, 834.
12. Han, Y.N., Xia, S.Q., Zhang, Y.Y., Zheng, J.H., and Li, W. (2017). Circular RNAs: A novel type of biomarker and genetic tools in cancer. *Oncotarget* 8, 64551–64563.
13. Hsiao, K.Y., Lin, Y.C., Gupta, S.K., Chang, N., Yen, L., Sun, H.S., and Tsai, S.J. (2017). Noncoding effects of circular RNA CCDC66 promote Colon Cancer growth and metastasis. *Cancer Res.* 77, 2339–2350.
14. Li, P., Lin, X.J., Yang, Y., Yang, A.K., Di, J.M., Jiang, Q.W., Huang, J.R., Yuan, M.L., Xing, Z.H., Wei, M.N., et al. (2019). Reciprocal regulation of miR-1205 and E2F1 modulates progression of laryngeal squamous cell carcinoma. *Cell Death Dis.* 10, 916.
15. Yang, Y., Ding, L., Li, Y., and Xuan, C. (2020). Hsa_circ_0039411 promotes tumorigenesis and progression of papillary thyroid cancer by miR-1179/ABCA9 and miR-1205/MTA1 signaling pathways. *J. Cell. Physiol.* 235, 1321–1329.
16. Yan, H., Chen, X., Li, Y., Fan, L., Tai, Y., Zhou, Y., Chen, Y., Qi, X., Huang, R., and Ren, J. (2019). MiR-1205 functions as a tumor suppressor by disconnecting the synergy between KRAS and MDM4/E2F1 in non-small cell lung cancer. *Am. J. Cancer Res.* 9, 312–329.
17. Yi, C., Li, H., Li, D., Qin, X., Wang, J., Liu, Y., Liu, Z., and Zhang, J. (2019). Upregulation of circular RNA circ_0034642 indicates unfavorable prognosis in glioma and facilitates cell proliferation and invasion via the miR-1205/BATF3 axis. *J. Cell. Biochem.* 120, 13737–13744.
18. Wu, X., Zhao, B., Cheng, Y., Yang, Y., Huang, C., Meng, X., Wu, B., Zhang, L., Lv, X., and Li, J. (2015). Melittin induces PTCH1 expression by down-regulating MeCP2 in human hepatocellular carcinoma SMMC-7721 cells. *Toxicol. Appl. Pharmacol.* 288, 74–83.
19. Li, Y., Zhu, Q., Tang, J., Guo, D.L., Duan, R., and Liu, J. (2018). MeCP2 level is associated with hepatocellular carcinoma development in chronic hepatitis B patients under antiviral therapy. *Int. J. Clin. Exp. Pathol.* 11, 1356–1364.
20. Zhao, L.Y., Zhang, J., Guo, B., Yang, J., Han, J., Zhao, X.G., Wang, X.F., Liu, L.Y., Li, Z.F., Song, T.S., and Huang, C. (2013). MECP2 promotes cell proliferation by activating ERK1/2 and inhibiting p38 activity in human hepatocellular carcinoma HEPG2 cells. *Cell. Mol. Biol. (Suppl)* 59, OL1876–OL1881.
21. Liu, H., Liu, Q.L., Zhai, T.S., Lu, J., Dong, Y.Z., and Xu, Y.F. (2020). Silencing miR-454 suppresses cell proliferation, migration and invasion via directly targeting MECP2 in renal cell carcinoma. *Am. J. Transl. Res.* 12, 4277–4289.
22. Zhang, X.Y., Xu, Y.Y., and Chen, W.Y. (2020). MicroRNA-1324 inhibits cell proliferative ability and invasiveness by targeting MECP2 in gastric cancer. *Eur. Rev. Med. Pharmacol. Sci.* 24, 4766–4774.